Cucurbituril as a container for assembling AIE aggregates

E. Y. Chernikova, M. A. Ustimova, O. V. Sulimova, Yu. V. Fedorov, O. A. Fedorova

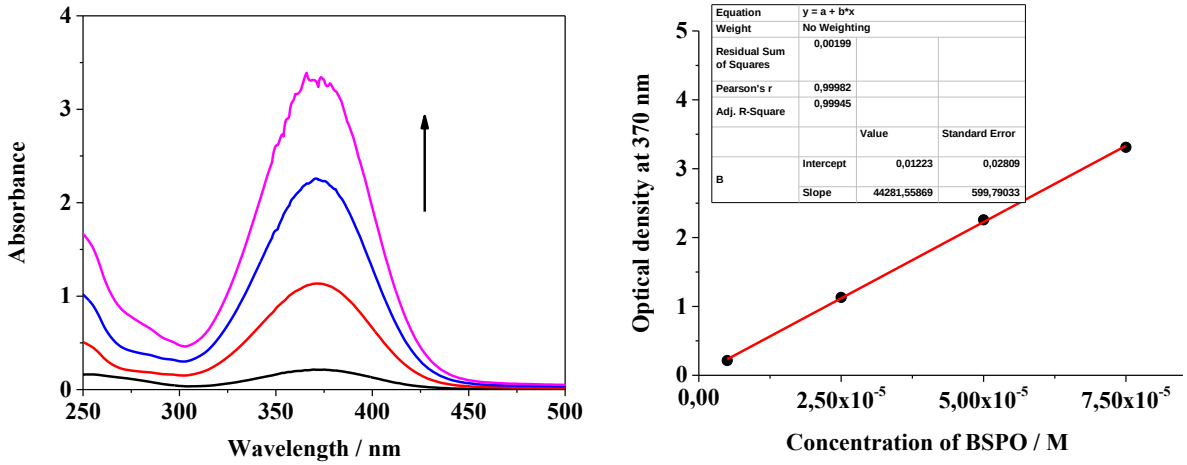


Figure S1. (a) Absorption spectra of **BSPO** dye at different concentrations C_{dye}= 5·10^{-6} M – black; C_{dye}= 2.5·10^{-5} M – red; C_{dye}= 5·10^{-5} M – blue; C_{dye}= 7.5·10^{-5} M – magenta; (b) linear dependence of optical density at λ_{abs}= 370 nm on the concentration of dye in aqueous solution.

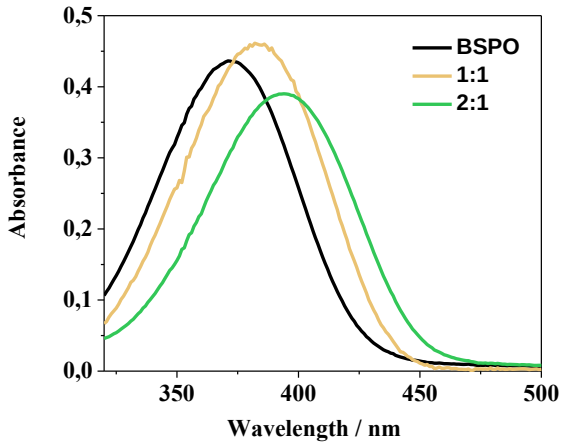


Figure S2. Absorption spectra of **BSPO** and its 1:1 and 2:1 CB[7] complexes calculated using Specfit/32 software.

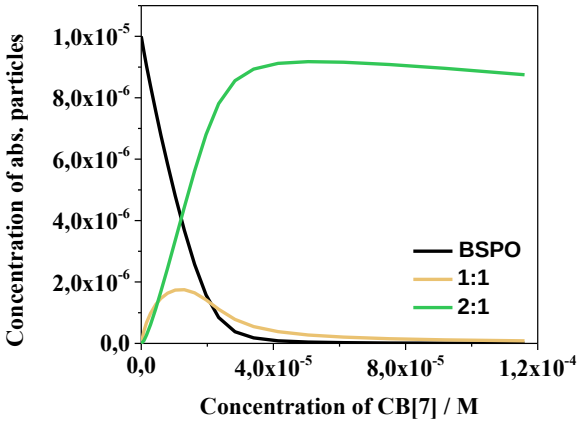


Figure S3. Concentrations of **BSPO** and its 1:1 and 2:1 CB[7] complexes as a function of CB[7] concentration in solution.

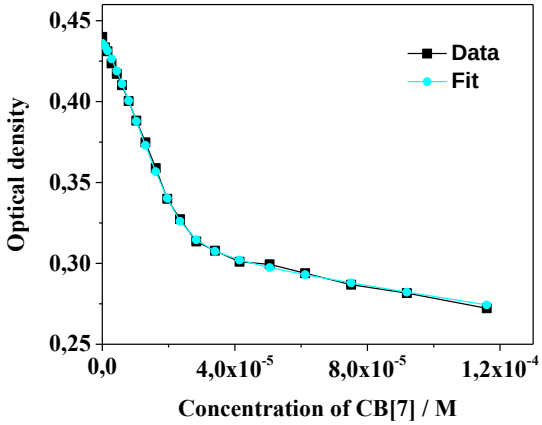


Figure S4. Calculated and experimental titration curves of **BSPO** with CB[7] at λ=372 nm.

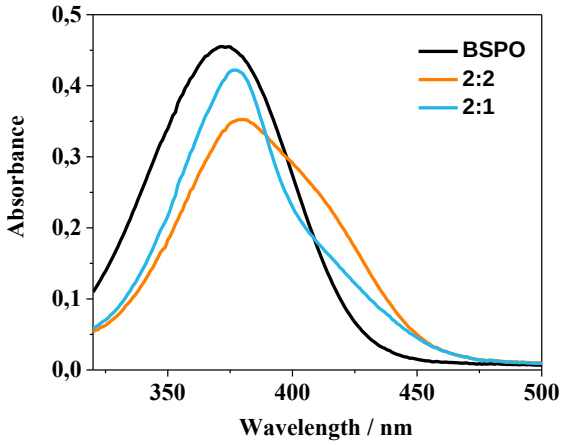


Figure S5. Absorption spectra of **BSPO** and its 2:2 and 2:1 CB[8] complexes calculated using Specfit/32 software.

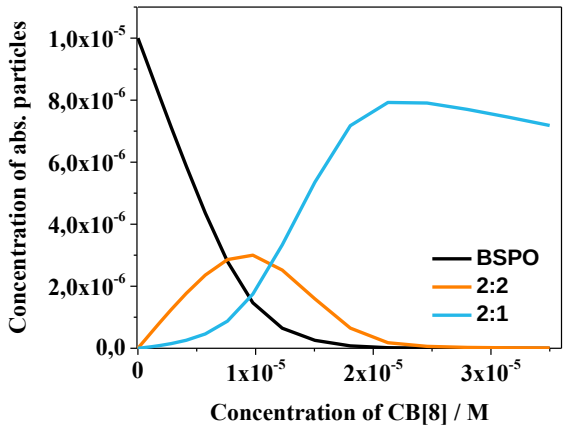


Figure S6. Concentrations of **BSPO** and its 1:1 and 2:1 CB[8] complexes as a function of CB[7] concentration.

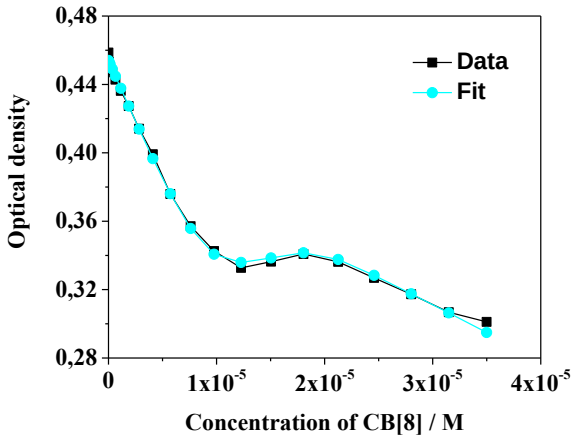


Figure S7. Calculated and experimental titration curves of **BSPO** with CB[8] at λ=372 nm.

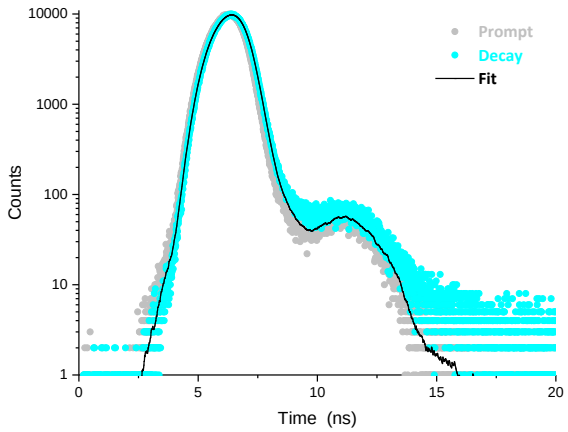


Figure S8. Time-resolved decay curves of **BSPO** ($C_{\mathbf{BSPO}} = 2 \cdot 10^{-5}$ M), H_2O, λ_{ex}=370 nm, λ_{em}=490 nm. The instrument response curve is marked in gray.

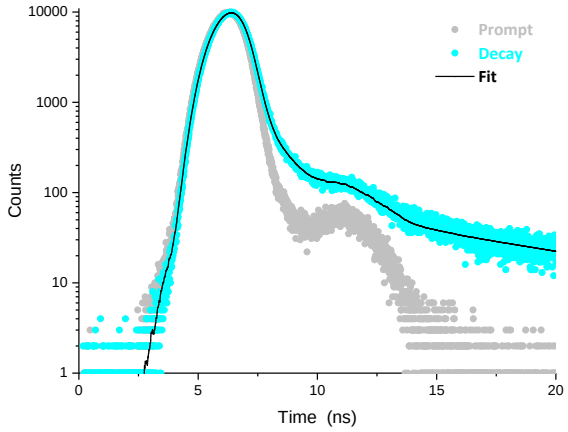


Figure S9. Time-resolved decay curves of **BSPO** ($C_{\mathbf{BSPO}}$ = 2·10^{-5} M) in the presence of 2 equiv. CB[7], H_2O, λ_{ex}=370 nm, λ_{em}=490 nm. The instrument response curve is shown in gray.

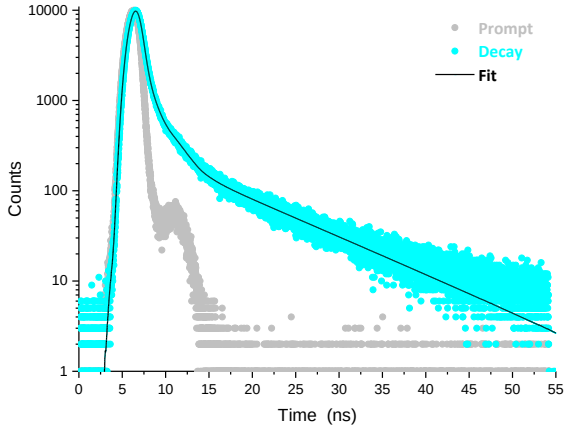


Figure S10. Time-resolved decay curves of **BSPO** ($C_{\mathbf{BSPO}}$ = 1·10^{-5} M) in the presence of 0.7 equiv. CB[8], H_2O, λ_{ex}=370 nm, λ_{em}=490 nm. The instrument response curve is marked in gray.

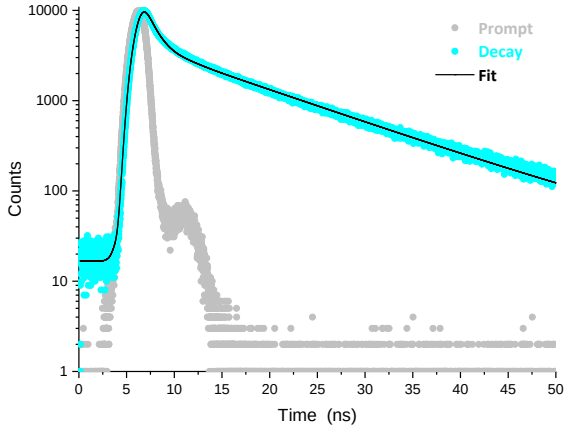


Figure S11. Time-resolved decay curves of **BSPO** ($C_{\mathbf{BSPO}}$ = 1·10^{-5} M) in the presence of 0.7 equiv. CB[8], H_2O, λ_{ex}=370 nm, λ_{em}=600 nm. The instrument response curve is marked in gray.

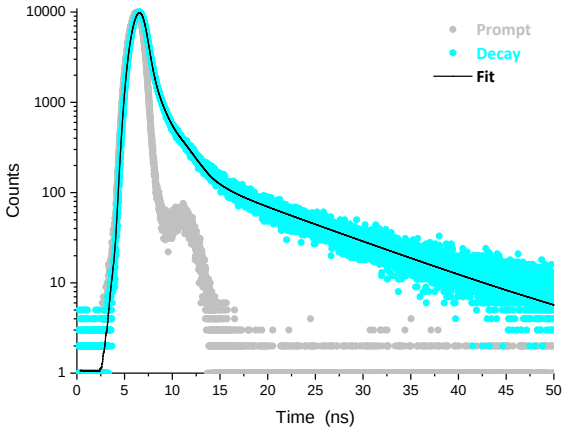


Figure S12. Time-resolved decay curves of **BSPO** ($C_{\mathbf{BSPO}}$ = $1 \cdot 10^{-5}$ M) in the presence of 12.25 equiv. CB[8], H_2O, λ_{ex}=370 nm, λ_{em}=490 nm. The instrument response curve is marked in gray.

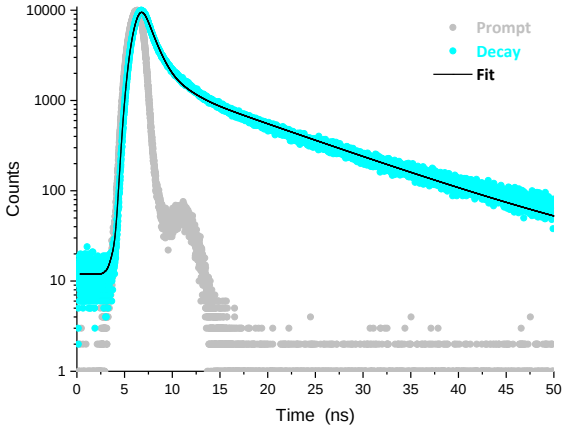


Figure S13. Time-resolved decay curves of **BSPO** ($C_{\mathbf{BSPO}}$ = $1 \cdot 10^{-5}$ M) in the presence of 12.25 equiv. CB[8], H_2O, λ_{ex}=370 nm, λ_{em}=600 nm. The instrument response curve is marked in gray.

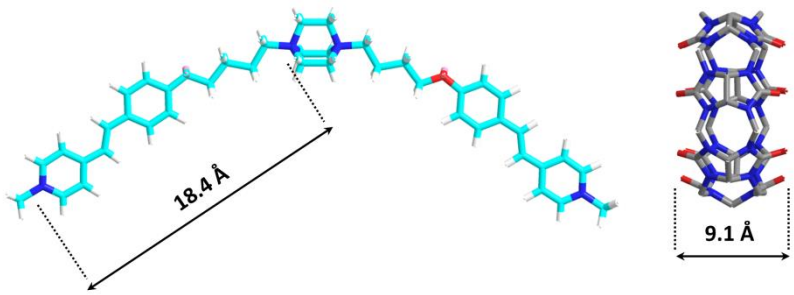


Figure S14. Optimized structures of **BSPO** and CB[7] dye by MMFF94 molecular mechanics.

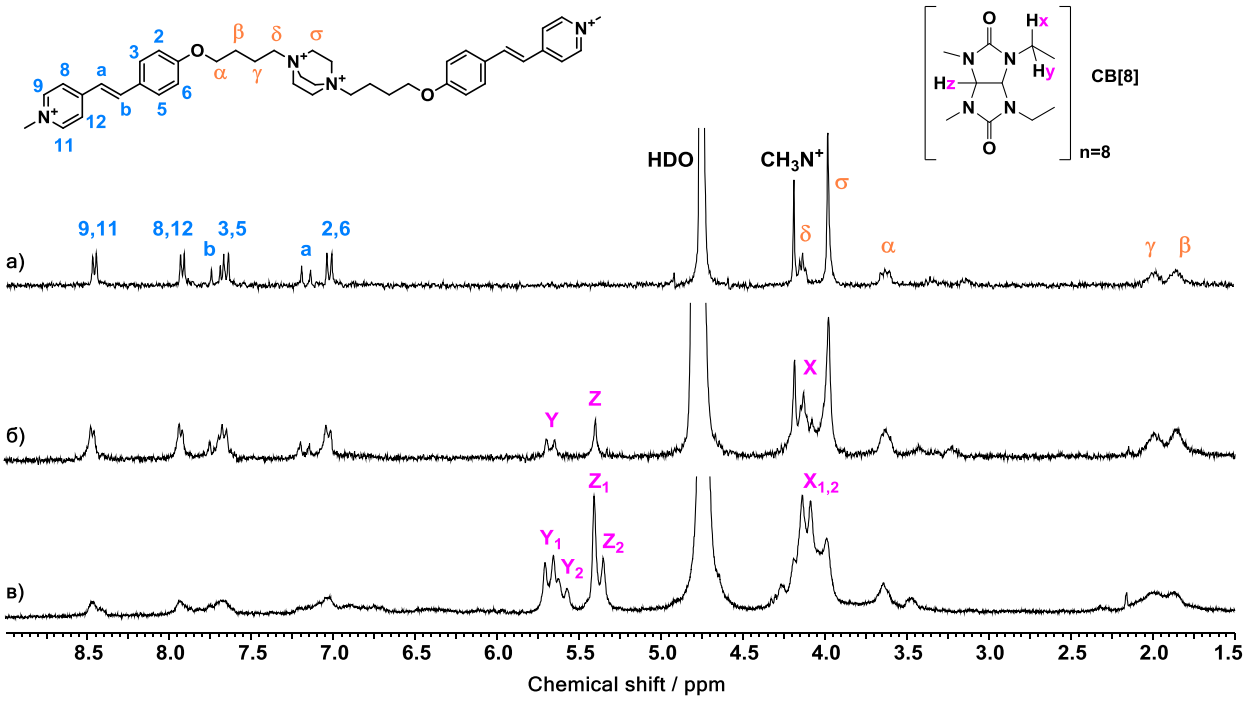


Figure S15. ^{1}H NMR spectra (400 MHz, 298 K, D_2O) of (a) **BSPO** dye (1.5 mM); dye at the ratio: (b) **BSPO**:CB[8] (1.5 mM/0.5 mM); (c) **BSPO**:CB[8] (1.5 mM/1 mM).

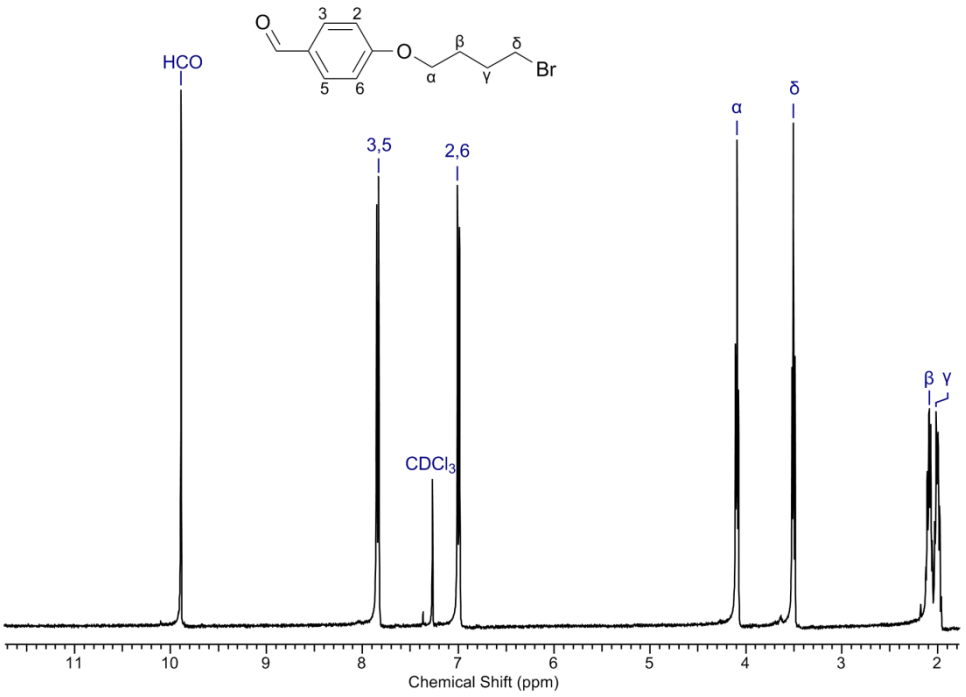


Figure S16. ^{1}H NMR spectrum **1** in $CDCl_3$.

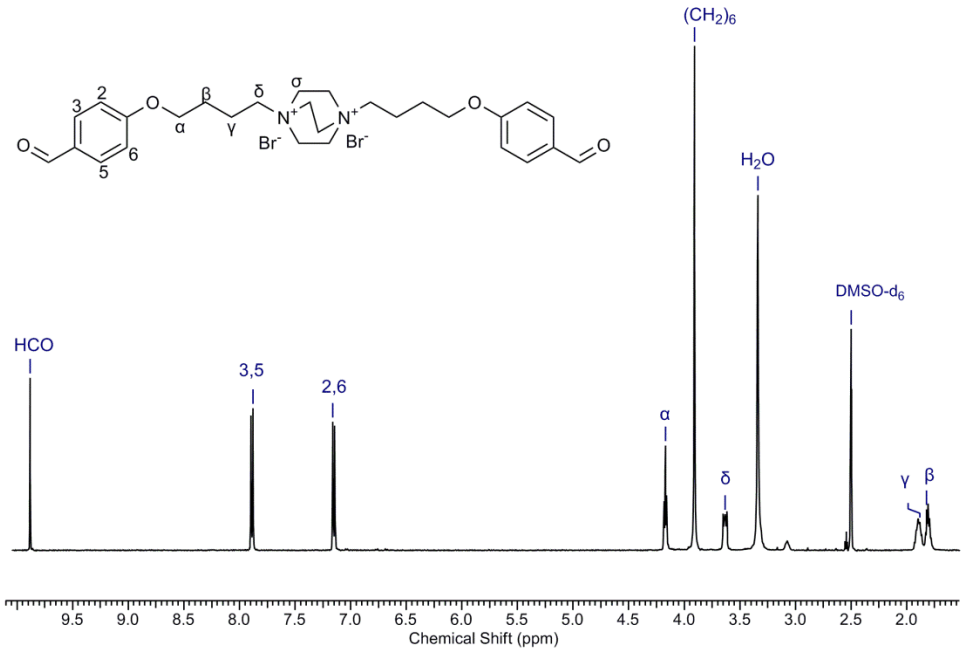


Figure S17. ^{1}H NMR spectrum of **2** in DMSO-d_6.

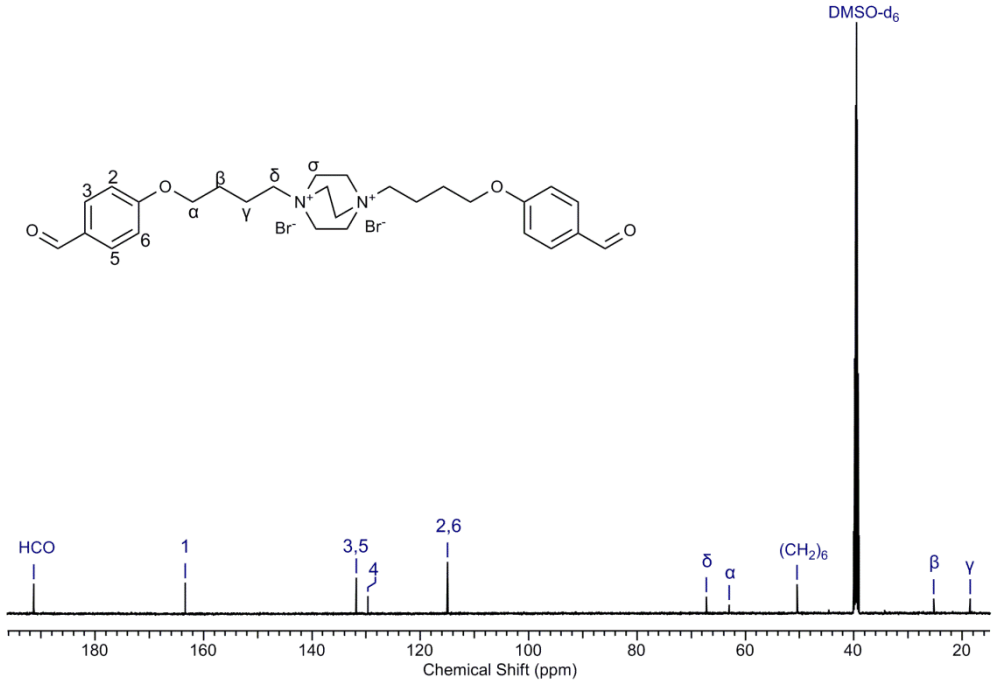


Figure S18. ^{13}C NMR spectrum of **2** in DMSO-d_6.

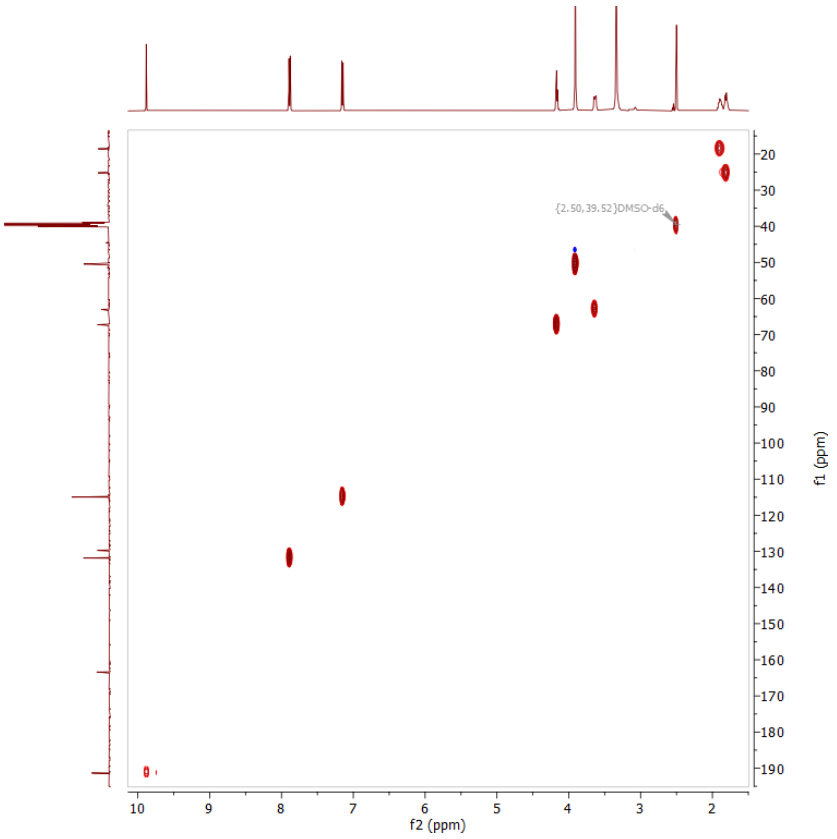


Figure S19. ^{1}H-^{13}C HSQC NMR spectrum of **2** in DMSO-d_6.

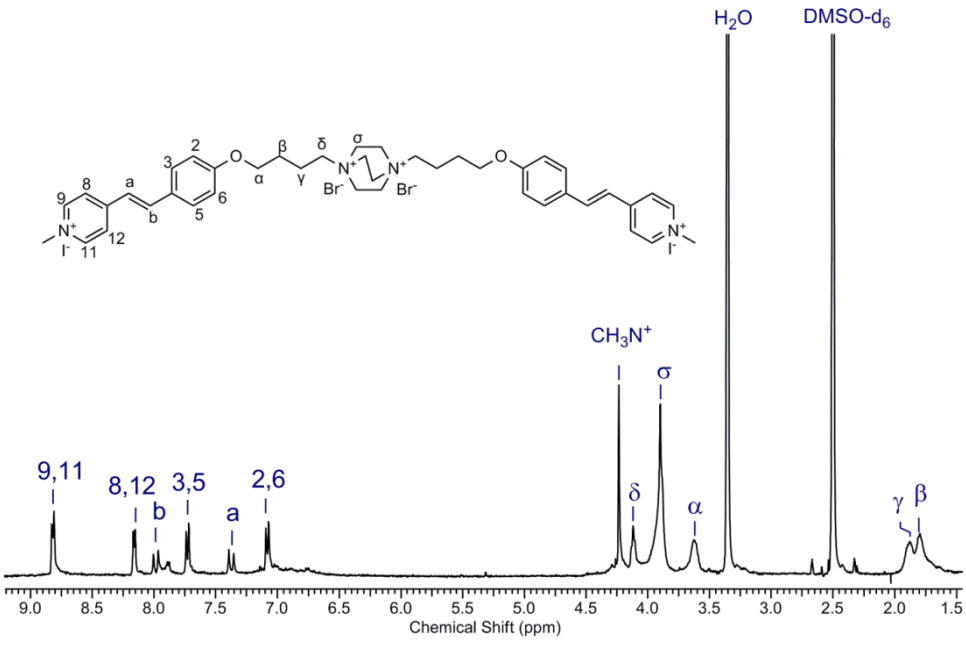


Figure S20. ^{1}H NMR spectrum of **BSPO** in DMSO-d_6.

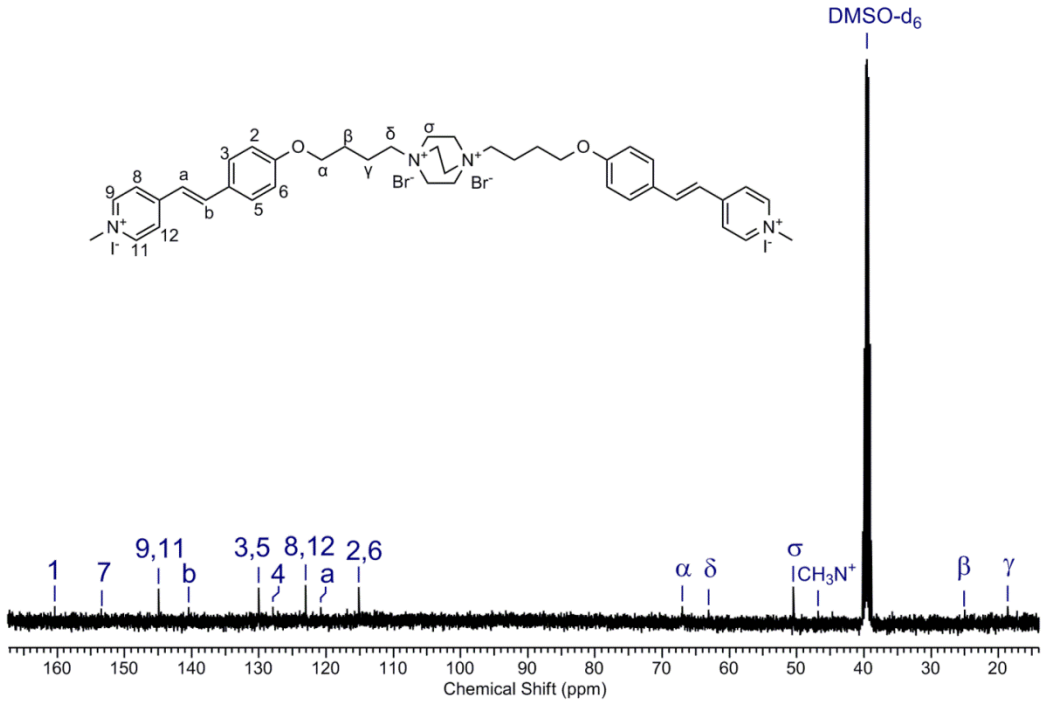


Figure S21. ^{13}C NMR spectrum of **BSPO** in DMSO-d_6.

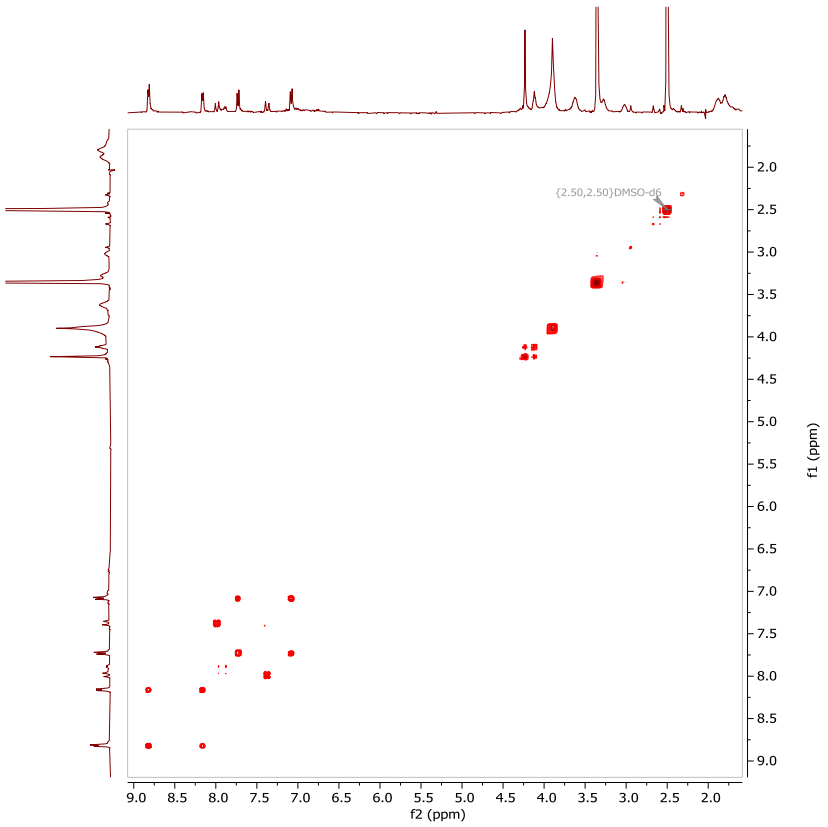


Figure S22. ^{1}H-^{1}H COSY NMR spectrum of **BSPO** in DMSO-d_6.

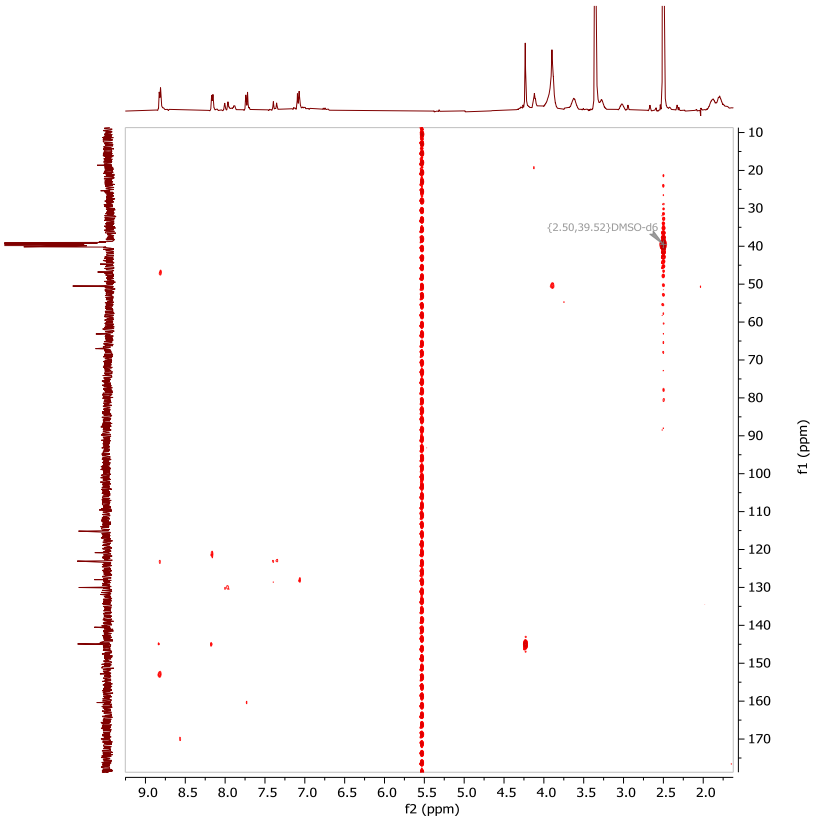


Figure S23. ^{1}H-^{13}C HMBC NMR spectrum of **BSPO** in DMSO-d_6.

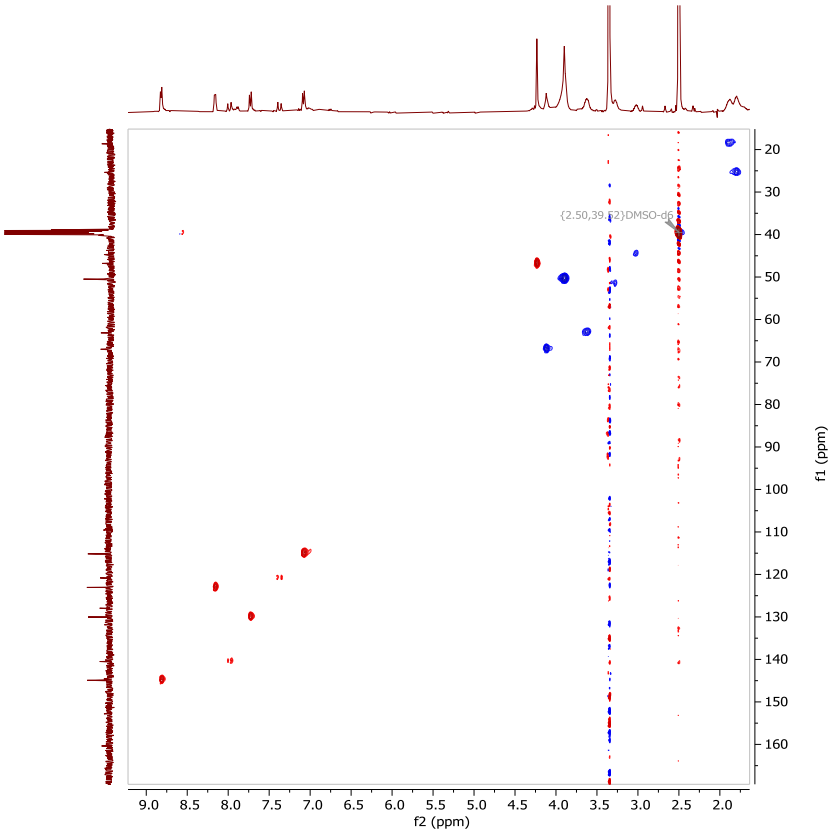


Figure S24. ^{1}H-^{13}C HSQC NMR spectrum of **BSPO** in DMSO-d_6.

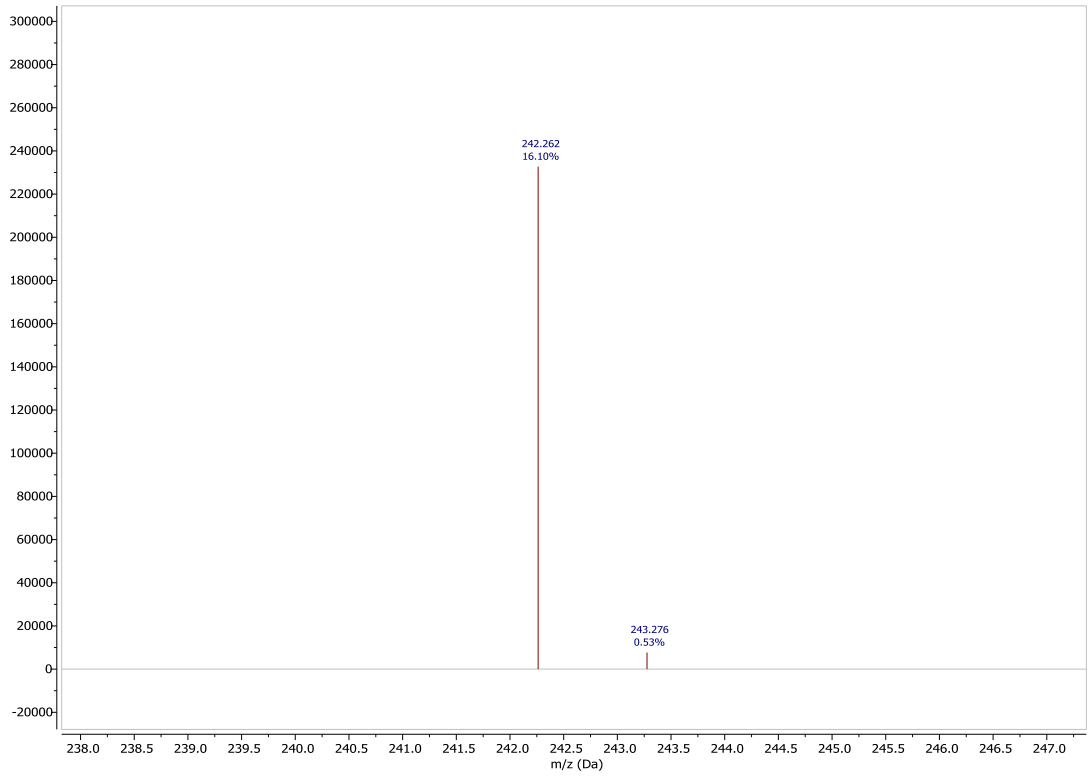


Figure S25. Mass spectrum of **BSPO** solution in MeOH (MALDI).